

Analysis of elastic wave scattering problems using volume integral equation method

Jungki Lee*

*Department of Mechano-Informatics and Design Engineering, Hongik University Jochiwon-Eup,
Yeonki-Gun, Chungnam, 339-701, South Korea*

(Manuscript Received June 12, 2007; Revised November 24, 2007; Accepted November 27, 2007)

Abstract

A volume integral equation method (VIEM) is applied for the effective analysis of elastic wave scattering problems in unbounded solids containing isotropic or anisotropic inclusions. It should be noted that this newly developed numerical method does not require Green's function for anisotropic inclusions to solve this class of problems since only Green's function for the unbounded isotropic matrix is involved in their formulation for the analysis. Through the analysis of plane wave scattering problems in unbounded isotropic matrix with isotropic or anisotropic inclusions, it will be established that this new method is very accurate and effective for solving plane wave scattering problems in unbounded solids containing isotropic or anisotropic inclusions.

Keywords: Elastic wave scattering; Volume integral equation method; VIEM

1. Introduction

Calculation of the stress and strain fields in solids containing multiple inclusions and subjected to external loads is of considerable interest in a variety of engineering applications. A notable example is the stress analysis of damaged fiber reinforced composites that consist of a large number of densely packed fibers with voids or cracks in the matrix. The matrix and the fibers in composites are usually made of isotropic material. However, some of the constituents can be anisotropic. As an example, in SiC/Ti metal matrix composites, the matrix is nearly isotropic, but the SiC fibers have strong anisotropy. Structural composites are often subject to manufacturing and/or service induced defects that strongly affect the remaining life of the structure. A precise knowledge of the deformation and stress fields near interacting isotropic or anisotropic fibers and voids/microcracks under remote loading can be extremely helpful in

predicting the failure and damage mechanisms in the composites. Several techniques have been proposed for analyzing multiple-inclusion interactions in an infinite medium (see e.g., [1-9]). However, none of these methods can be applied to the general problem in which the inclusions or voids are of arbitrary shape and their concentration is high. To our knowledge the only available methods to solve problems of this type are the finite element (FEM) or the boundary integral equation (BIEM) method.

However, the finite element method is most effective when the domain of the problem is finite and it is often not possible to separate the influence of the boundary from that of the "microscopic" features of the material on the elastic field. Conventional finite element methods cannot be directly applied to infinite domains. The boundary integral equation method is, in principle, applicable to this class of problems since it can be applied to infinite domains. However, since Green's function for anisotropic inclusions is involved in the boundary integral equation method and Green's function for an anisotropic material is much more complex than that for isotropic material, their numeri-

*Corresponding author. Tel.: +82 41 860 2619, Fax.: +82 41 866 9129
E-mail address: inq3jkl@wow.hongik.ac.kr
DOI 10.1007/s12206-007-1113-7

cal treatment of the boundary integral equations becomes extremely cumbersome (see e.g., [10-13]).

In this paper the solution of the general inhomogeneous elastodynamic problem is formulated by means of a volume integral equation method for the effective accurate calculation of the stresses and displacements in unbounded isotropic solids in presence of multiple isotropic or anisotropic inclusions.

It should be noted that this newly developed numerical method does not require Green's function for anisotropic inclusions, and it can also be applied to general two-dimensional elastodynamic as well as elastostatic problems (see e.g., [14, 15]) for arbitrary geometry and number of inhomogeneities. In the formulation of the method, the continuity condition at each interface is automatically satisfied, and in contrast to finite element method, where the full domain needs to be discretized, this method requires discretization of the inclusions only. Finally, the method takes full advantage of the pre- and post-processing capabilities developed in FEM and BIEM.

In this paper, a detailed analysis of the displacement and stress fields is carried out for an unbounded isotropic matrix containing isotropic or orthotropic cylindrical inclusions. The field at infinity is assumed to be a plane time harmonic elastic wave propagating parallel to the x-axis. The incident wave can be P waves with particle motion along the x-axis, SV waves with particle motion parallel to the y-axis, or SH waves with particle motion parallel to the z-axis. The accuracy and effectiveness of the new method are examined through comparison with results obtained from analytical and boundary integral equation methods. It is demonstrated that this new method is very accurate and effective for solving plane elastodynamic problems in unbounded solids containing isotropic or anisotropic inclusions.

2. The volume integral equation method (VIEM)

The geometry of the general elastodynamic problem is shown in Fig. 1. Let ρ and c_{ijkl} denote the density and the elastic tensor of the solid. Let $\rho^{(1)}$ and $c_{ijkl}^{(1)}$ denote the density and the elastic stiffness tensor of the inclusion and $\rho^{(2)}$ and $c_{ijkl}^{(2)}$ those of the unbounded matrix material. The matrix is assumed to be homogeneous and isotropic so that $c_{ijkl}^{(2)}$ is a constant isotropic tensor, while $c_{ijkl}^{(1)}$ is arbitrary, i.e., the inclusions may, in general, be inhomogeneous and anisot-

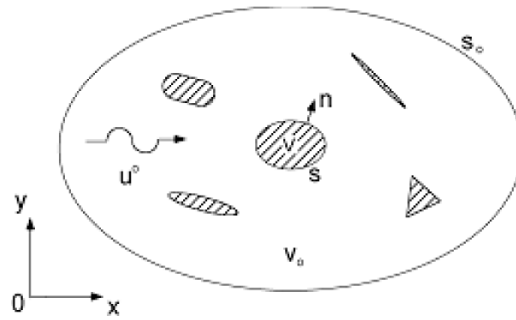


Fig. 1. Geometry of the general elastodynamic problem.

ropic. The interfaces between the inclusions and the matrix are assumed to be perfectly bonded, insuring continuity of the displacement and stress vectors.

Let $e^{-i\omega t} u_m^o(x, \omega)$ denote the m th component of the displacement vector due to the incident field at x in absence of the inclusions and let $e^{-i\omega t} u_m(x, \omega)$ denote the same in presence of the inclusions, where ω is the circular frequency of the waves. In what follows the common time factor $e^{-i\omega t}$ and the explicit dependence on ω of all field quantities will be suppressed.

It has been shown by Mal and Knopoff [16] that $u_m(x)$ satisfies the equation

$$u_m = u_m^o(x) + \int_V [\delta\rho\omega^2 g_i^m(\xi, x) u_i(\xi) - \delta c_{ijkl} \xi_{i,j}^m(\xi, x) u_{k,l}(\xi)] d\xi \quad (1)$$

where the integral is over the whole space, $\delta\rho$ and δc_{ijkl} are the contrasts in the density and elastic tensor of the inclusions and the matrix; i.e., $\delta\rho = \rho^{(1)} - \rho^{(2)}$ and $\delta c_{ijkl} = c_{ijkl}^{(1)} - c_{ijkl}^{(2)}$, and $g_i^m(\xi, x)e^{-i\omega t}$ is Green's function for the unbounded homogeneous matrix material; i.e., $g_i^m(\xi, x)e^{-i\omega t}$ represents the i th component of the displacement at ξ due to a concentrated force, $e_m e^{-i\omega t}$, at x in the m th direction. In Eq. (1) the summation convention and comma notation have been used and the differentiations are with respect to the integration variable, ξ_j . It should be noted that the integrand is non-zero within the inclusions only, since $\delta c_{ijkl} = 0$, outside the inclusions.

If $x \in \mathbf{R}$ (within the inclusions), then Eq. (1) is an integrodifferential equation for the unknown displacement vector $\mathbf{u}(x)$; it can, in principle, be determined through the solution of Eq. (1). An algorithm based on the discretization of Eq. (1) was developed by Lee and Mal [17, 18] to calculate numerically the

unknown displacement vector $\mathbf{u}(\mathbf{x})$ by discretizing the inclusions using standard finite elements. Once $\mathbf{u}(\mathbf{x})$ within the inclusions is determined, the displacement field outside the inclusions can be obtained from Eq. (1) by evaluating the integral, and the stress field within and outside the inclusions can also be determined without any difficulty. The details of the numerical treatment of Eq. (1) can be found in Lee and Mal [17, 18] and will be omitted. In Eq. (1), $g_i^m(\xi, \mathbf{x})e^{-i\omega t}$ is Green's function for the unbounded isotropic matrix material. Thus, the volume integral equation method does not require the use of Green's function for the anisotropic material of the inclusions. This is in contrast to the boundary integral equation method, where the infinite medium Green's functions for both the matrix and the inclusion are involved in the formulation of the equations. The Green's functions for anisotropic solids can only be obtained in integral forms and their evaluation in the vicinity of the source point is very difficult. Since the numerical implementation of conventional boundary integral equation (BIE) requires the evaluation of the displacements and stresses associated with Green's function at a large number of points, the method becomes extremely unwieldy, if not impossible, to apply in even the simplest of model geometries. The present method is free from this problem.

3. Scattering of P and SV waves

3.1 Scattering of P and SV waves in unbounded isotropic matrix containing an isotropic inclusion

In order to check the accuracy of the volume integral equation method, we first consider a single isotropic cylindrical inclusion in the unbounded isotropic matrix. The incident wave can be a P wave with particle motion along the x-axis, or an SV wave with particle motion parallel to the y-axis. Let ρ_1 and λ_1, μ_1 denote the density and Lamé constants of the isotropic inclusion, and ρ_2 and λ_2, μ_2 the density and Lamé constants of the isotropic matrix, respectively.

For P and SV waves, the volume integral equation (1) reduces to

$$u_1(\mathbf{x}) = u_1^0(\mathbf{x}) + \int_R \{ \delta\rho\omega^2 [g_1^1(\xi, \mathbf{x})u_1(\xi) + g_2^1(\xi, \mathbf{x})u_2(\xi)] - [\delta(\lambda + 2\mu)g_{1,1}^1u_{1,1} + \delta\lambda g_{1,1}^1u_{1,1}] \} d\xi_1 d\xi_2 \quad (2)$$

$$- [\delta\mu g_{1,2}^1(u_{1,2} + u_{2,1}) + \delta(\lambda + 2\mu)g_{2,2}^1u_{2,2}] - [\delta\lambda g_{2,2}^1u_{1,1} + \delta\mu g_{2,1}^1(u_{1,2} + u_{2,1})] \} d\xi_1 d\xi_2$$

and

$$u_2(\mathbf{x}) = u_2^0(\mathbf{x}) + \int_R \{ \delta\rho\omega^2 [g_1^2(\xi, \mathbf{x})u_1(\xi) + g_2^2(\xi, \mathbf{x})u_2(\xi)] - [\delta(\lambda + 2\mu)g_{1,1}^2u_{1,1} + \delta\lambda g_{1,1}^2u_{2,2}] - [\delta\mu g_{1,2}^2(u_{1,2} + u_{2,1}) + \delta(\lambda + 2\mu)g_{2,2}^2u_{2,2}] - [\delta\lambda g_{2,2}^2u_{1,1} + \delta\mu g_{2,1}^2(u_{1,2} + u_{2,1})] \} d\xi_1 d\xi_2 \quad (3)$$

where $u_1(\mathbf{x}), u_2(\mathbf{x})$ are the in-plane displacement components, $\delta\rho = \rho_1 - \rho_2$, $\delta(\lambda + 2\mu) = (\lambda_1 + 2\mu_1) - (\lambda_2 + 2\mu_2)$, $\delta\lambda = \lambda_1 - \lambda_2$, and $\delta\mu = \mu_1 - \mu_2$.

In Eqs. (2) and (3), $g_i^m(\xi, \mathbf{x})$ is Green's function for the unbounded isotropic matrix material. The Green's function for the two-dimensional time-harmonic elastodynamic state is given by (Kitahara, 1985)

$$g_2^1 = \frac{i}{4\rho\omega^2} \left\{ \frac{(x_1 - \xi_1)(x_2 - \xi_2)}{r^2} k_1^2 H_0(k_1 r) - \frac{(x_1 - \xi_1)(x_2 - \xi_2)}{r^2} k_2^2 H_0(k_2 r) - \frac{2(x_1 - \xi_1)(x_2 - \xi_2)}{r^3} k_1 H_1(k_1 r) - \frac{2(x_1 - \xi_1)(x_2 - \xi_2)}{r^3} k_2 H_1(k_2 r) \right\}$$

$$g_1^2 = g_2^1$$

$$g_1^1 = \frac{i}{4\rho\omega^2} \left\{ \frac{(x_1 - \xi_1)^2}{r^2} k_1^2 H_0(k_1 r) - \frac{(x_1 - \xi_1)^2}{r^2} k_2^2 H_0(k_2 r) + \frac{1}{r} \left[1 - 2 \frac{(x_1 - \xi_1)^2}{r^2} \right] k_1 H_1(k_1 r) - \frac{1}{r} \left[1 - 2 \frac{(x_1 - \xi_1)^2}{r^2} \right] k_2 H_1(k_2 r) + k_2^2 H_0(k_2 r) \right\} \quad (4)$$

$$g_2^2 = \frac{i}{4\rho\omega^2} \left\{ \frac{(x_2 - \xi_2)^2}{r^2} k_1^2 H_0(k_1 r) \right\}$$

$$\begin{aligned}
 & -\frac{(x_2 - \xi_2)^2}{r^2} k_2^2 H_0(k_2 r) \\
 & + \frac{1}{r} \left[1 - 2 \frac{(x_2 - \xi_2)^2}{r^2} \right] k_1 H_1(k_1 r) \\
 & + \frac{1}{r} \left[1 - 2 \frac{(x_2 - \xi_2)^2}{r^2} \right] - k_2 H_1(k_2 r) \\
 & + k_2^2 H_0(k_2 r) \}
 \end{aligned}$$

where $r = |\mathbf{x} - \boldsymbol{\xi}|$, and H_0 and H_1 are the Hankel functions of the first kind of the zeroth and first orders, and $k_1 = \omega/\alpha_2$, $k_2 = \omega/\beta_2$ are the P and S wavenumbers, and α_2 , β_2 are the longitudinal and shear wave speeds in the unbounded matrix.

Finite element discretization of the inclusions in Eqs. (2) and (3) results in a system of two coupled system of linear algebraic equations for the unknown nodal displacements inside the inclusion. Once the displacement field, $\mathbf{u}(\mathbf{x})$, within the inclusion is determined, that outside the inclusions can be obtained from Eqs. (2) and (3) by evaluating the integrals. The stress field within and outside the inclusions can also be determined without any difficulty. The details of the numerical treatment can be found in Lee and Mal [17, 18] and will be omitted.

3.2 Scattering of P and SV waves in unbounded isotropic matrix containing an orthotropic inclusion

3.2.1 The volume integral equation method (VIEM)

Consider a single orthotropic cylindrical inclusion in the unbounded isotropic matrix. The incident wave can be either a P wave or an SV wave. Let the coordinate axes $x_1(x)$, $x_2(y)$, $x_3(z)$, be taken parallel to the symmetry axes of the orthotropic material. Let ρ_1 , and c_{11} , c_{12} , c_{22} , c_{66} denote the density and elastic constants of the inclusion, and ρ_2 and λ_2 , μ_2 the density and Lamé constants of the isotropic matrix, respectively.

For P and SV waves, the volume integral equation (1) reduces to

$$\begin{aligned}
 u_1(\mathbf{x}) = & u_1^0(\mathbf{x}) \\
 & + \int_R \{ \delta \rho \omega^2 [g_1^1(\boldsymbol{\xi}, \mathbf{x}) u_1(\boldsymbol{\xi}) + g_2^1(\boldsymbol{\xi}, \mathbf{x}) u_2(\boldsymbol{\xi})] \\
 & - [\delta c_{11} g_{1,1}^1 u_{1,1} + \delta c_{12} g_{1,1}^1 u_{2,2}] \\
 & - [\delta c_{66} g_{1,2}^1 (u_{1,2} + u_{2,1}) + \delta c_{22} g_{2,2}^1 u_{2,2}] \\
 & - [\delta c_{12} g_{2,2}^1 u_{1,1} + \delta c_{66} g_{2,1}^1 (u_{1,2} + u_{2,1})] \} d\xi_1 d\xi_2
 \end{aligned} \tag{5}$$

and

$$\begin{aligned}
 u_2(\mathbf{x}) = & u_2^0(\mathbf{x}) + \int_R \{ \delta \rho \omega^2 [g_1^2(\boldsymbol{\xi}, \mathbf{x}) u_1(\boldsymbol{\xi}) + g_2^2(\boldsymbol{\xi}, \mathbf{x}) u_2(\boldsymbol{\xi})] \\
 & - [\delta c_{11} g_{1,1}^2 u_{1,1} + \delta c_{12} g_{1,1}^2 u_{2,2}] \\
 & - [\delta c_{66} g_{1,2}^2 (u_{1,2} + u_{2,1}) + \delta c_{22} g_{2,2}^2 u_{2,2}] \\
 & - [\delta c_{12} g_{2,2}^2 u_{1,1} + \delta c_{66} g_{2,1}^2 (u_{1,2} + u_{2,1})] \} d\xi_1 d\xi_2
 \end{aligned} \tag{6}$$

where $u_1(\mathbf{x})$, $u_2(\mathbf{x})$ are the in-plane displacement components, $\delta \rho = \rho_1 - \rho_2$, $\delta c_{11} = c_{11} - (\lambda_2 + 2\mu_2)$, $\delta c_{12} = c_{12} - \lambda_2$, $\delta c_{22} = c_{22} - (\lambda_2 + 2\mu_2)$, and $\delta c_{66} = c_{66} - \mu_2$.

In Eqs. (5) and (6), g_i^m is Green's function for the unbounded isotropic matrix material. Thus, the volume integral equation method does not require the use of Green's function for the anisotropic material of the inclusions. This is in contrast to the boundary integral equation method, where the infinite medium Green's functions for both the matrix and the inclusion are involved in the formulation of the equations.

Finite element discretization of the inclusions in Eqs. (5) and (6) results in a system of two coupled system of linear algebraic equations for the unknown nodal displacements inside the inclusion. Once the displacement field, $\mathbf{u}(\mathbf{x})$, within the inclusion is determined, that outside the inclusions can be obtained from Eqs. (5) and (6) by evaluating the integrals. The stress field within and outside the inclusions can also be determined without any difficulty.

3.2.2 The boundary integral equation method (BIEM)

The integral equation on the outer surface S_+ of the anisotropic inclusion can be expressed as (Banerjee [20], Rizzo et al. [21])

$$\begin{aligned}
 u_m(\mathbf{x}) = & u_m^o(\mathbf{x}) + c_{ijkl}^{(M)} \int_{S_+} [g_{k,l}^{m(M)}(\boldsymbol{\xi}, \mathbf{x}) u_i(\boldsymbol{\xi}) \\
 & - g_i^{m(M)}(\boldsymbol{\xi}, \mathbf{x}) u_{k,l}(\boldsymbol{\xi})] n_j ds
 \end{aligned} \tag{7}$$

while for the interior surface S_-

$$\begin{aligned}
 u_m(\mathbf{x}) = & -c_{ijkl}^{(I)} \int_{S_-} [g_{k,l}^{m(I)}(\boldsymbol{\xi}, \mathbf{x}) u_i(\boldsymbol{\xi}) \\
 & - g_i^{m(I)}(\boldsymbol{\xi}, \mathbf{x}) u_{k,l}(\boldsymbol{\xi})] n_j ds
 \end{aligned} \tag{8}$$

In Eqs. (7) and (8) n is the outward unit normal to S_+ , and the superscripts (M) and (I) indicate that the quantities involved are for the isotropic matrix and

the inclusions, respectively. Eqs. (7) and (8), together with the continuity conditions across \mathcal{S} , give rise to the boundary integral equation for $\mathbf{u}(\mathbf{x})$. When the inclusion becomes a void, the integral equations reduce to the standard boundary integral equation

$$u_m(\mathbf{x}) = u_m^o(\mathbf{x}) + c_{ijkl}^{(M)} \int_{\mathcal{S}} g_{k,l}^{m(M)}(\xi, \mathbf{x}) u_i(\xi) n_j ds \quad (9)$$

Consider a single orthotropic cylindrical inclusion in the unbounded isotropic matrix. The incident wave can be either a P wave or an SV wave. Let ρ_1 and $c_{11}, c_{12}, c_{22}, c_{66}$ denote the density and elastic constants of the inclusion, respectively, and ρ_2 and λ_2, μ_2 being the density and Lamé constants of the isotropic matrix, respectively.

The integral equations on the outer surface of the orthotropic inclusion can be expressed as

$$\begin{aligned} u_1(\mathbf{x}) &= u_1^o(\mathbf{x}) \\ &- \int_{\mathcal{S}_+} \{ [g_1^{1(M)}(\xi, \mathbf{x}) t_1(\xi) + g_2^{1(M)}(\xi, \mathbf{x}) t_2(\xi)] \\ &- [T_1^{1(M)}(\xi, \mathbf{x}) u_1(\xi) - T_2^{1(M)}(\xi, \mathbf{x}) u_2(\xi)] \} dS(\xi) \\ u_2(\mathbf{x}) &= u_2^o(\mathbf{x}) \\ &- \int_{\mathcal{S}_+} \{ [g_1^{2(M)}(\xi, \mathbf{x}) t_1(\xi) + g_2^{2(M)}(\xi, \mathbf{x}) t_2(\xi)] \\ &- [T_1^{2(M)}(\xi, \mathbf{x}) u_1(\xi) - T_2^{2(M)}(\xi, \mathbf{x}) u_2(\xi)] \} dS(\xi) \end{aligned} \quad (10)$$

where $g_{\alpha}^{\beta(M)}$ is Green's function for the unbounded isotropic matrix material and is given in Eq. (4). $T_{\alpha}^{\beta(M)}$ ($\alpha, \beta = 1, 2$) and t_{α} are given by

$$\begin{aligned} T_1^{1(M)} &= (\lambda + 2\mu) g_{1,1}^{1(M)} n_1 + \lambda g_{2,2}^{1(M)} n_1 + \mu (g_{1,2}^{1(M)} + g_{2,1}^{1(M)}) n_2, \\ T_1^{2(M)} &= (\lambda + 2\mu) g_{1,1}^{2(M)} n_1 + \lambda g_{2,2}^{2(M)} n_1 + \mu (g_{1,2}^{2(M)} + g_{2,1}^{2(M)}) n_2, \\ T_2^{1(M)} &= (\lambda + 2\mu) g_{2,2}^{1(M)} n_2 + \lambda g_{1,1}^{1(M)} n_2 + \mu (g_{1,2}^{1(M)} + g_{2,1}^{1(M)}) n_1, \\ T_2^{2(M)} &= (\lambda + 2\mu) g_{2,2}^{2(M)} n_2 + \lambda g_{1,1}^{2(M)} n_2 + \mu (g_{1,2}^{2(M)} + g_{2,1}^{2(M)}) n_1 \end{aligned} \quad (11)$$

and

$$\begin{aligned} t_1 &= (\lambda + 2\mu) u_{1,1} n_1 + \lambda u_{2,2} n_1 + \mu (u_{1,2} + u_{2,1}) n_2, \\ t_2 &= (\lambda + 2\mu) u_{2,2} n_2 + \lambda u_{1,1} n_2 + \mu (u_{1,2} + u_{2,1}) n_1 \end{aligned} \quad (12)$$

For the interior surface, the equations are

$$\begin{aligned} u_1(\mathbf{x}) &= \int_{\mathcal{S}_-} \{ [g_1^{1(I)}(\xi, \mathbf{x}) t_1(\xi) + g_2^{1(I)}(\xi, \mathbf{x}) t_2(\xi)] \\ &- [T_1^{1(I)}(\xi, \mathbf{x}) u_1(\xi) - T_2^{1(I)}(\xi, \mathbf{x}) u_2(\xi)] \} dS(\xi) \\ u_2(\mathbf{x}) &= \int_{\mathcal{S}_-} \{ [g_1^{2(I)}(\xi, \mathbf{x}) t_1(\xi) + g_2^{2(I)}(\xi, \mathbf{x}) t_2(\xi)] \\ &- [T_1^{2(I)}(\xi, \mathbf{x}) u_1(\xi) - T_2^{2(I)}(\xi, \mathbf{x}) u_2(\xi)] \} dS(\xi) \end{aligned} \quad (13)$$

It should be noted that $g_{\alpha}^{\beta(I)}$ and $T_{\alpha}^{\beta(I)}$ ($\alpha, \beta = 1, 2$) in Eq. (13) are Green's function and their associated tractions for the orthotropic inclusions. And t_{α} is given by

$$\begin{aligned} t_1 &= c_{11} u_{1,1} n_1 + c_{12} u_{2,2} n_1 + c_{66} (u_{1,2} + u_{2,1}) n_2 \\ t_2 &= c_{22} u_{2,2} n_2 + c_{12} u_{1,1} n_2 + c_{66} (u_{1,2} + u_{2,1}) n_1 \end{aligned} \quad (14)$$

However, the closed form solution for the two-dimensional time-harmonic elastodynamic Green's function for the orthotropic material is not available in the literature [10-12]. Therefore, the numerical implementation of the boundary element method for the solving wave scattering by anisotropic inclusions is an extremely difficult if not impossible task.

3.2.3 Numerical formulation

It should be noted that the volume integral equation method involves only $g_{\alpha}^{\beta(M)}$ and $T_{\alpha}^{\beta(M)}$ for the isotropic matrix, while the boundary integral equation involves $g_{\alpha}^{\beta(M)}$ and $T_{\alpha}^{\beta(I)}$ for the anisotropic inclusions in addition to these. Furthermore, the singularities in VIEM are weaker (integrable) than those in BIEM, where they are of the Cauchy type. We have used the direct integration scheme as introduced by Cerrolaza and Alarcon [22], Li and Han [23] and Lu and Ye [24] after suitable modifications to handle the singularities; a description of the modified method used in the discretization of the volume integral equation is given by Lee and Mal [17, 18].

4. Single inclusion problems

4.1 Scattering of P waves in unbounded isotropic matrix containing an isotropic inclusion

We first consider a single isotropic cylindrical inclusion in the unbounded isotropic matrix as shown in Fig. 2. Fig. 3 shows a typical discretized model used

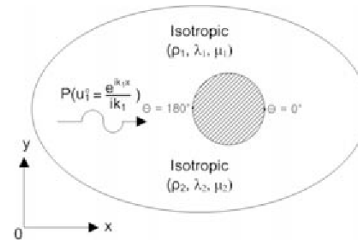


Fig. 2 P wave interaction with an isotropic inclusion in unbounded isotropic matrix.

Table 1 Material properties of the isotropic matrix and the orthotropic and isotropic inclusion.

Elastic constants	Isotropic matrix	Orthotropic inclusion	Isotropic inclusion
ρ (g/cm ³)	4.54	2.78	2.78
λ (GPa)	67.34	-	93.03
μ (GPa)	37.88	-	93.03
c_{11} (GPa)	143.10	279.08	279.09
c_{12} (GPa)	67.34	7.80	93.03
c_{22} (GPa)	143.10	30.56	279.09
c_{66} (GPa)	37.88	11.80	93.03

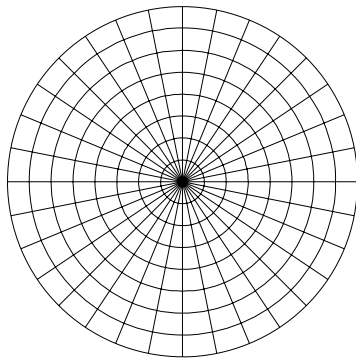


Fig. 3. A typical discretized model in the volume integral equation method.

in the VIEM. The standard eight-node quadrilateral and six-node triangular elements were used in the VIEM. In the unbounded isotropic matrix $\delta\rho$, $\delta(\lambda + 2\mu)$, and $\delta\mu$ vanish, so that, it is necessary to discretize the isotropic inclusion only. The total number of elements used in VIEM was 256.

In the P wave case the incident wave is assumed to be given by

$$u_1^o = \frac{e^{ik_1x}}{ik_1} \tag{15}$$

where k_1 is the P wave number in the matrix material. The elastic constants for the materials of the isotropic matrix and the isotropic inclusion are listed in Table 1. The calculations are carried out for three different normalized wavenumbers, $k_1a = 1.25, 3.0,$ and $5.0,$ corresponding to wavelengths to inclusion radius ratios between about 0.2 and 0.8. This is a useful range of frequencies for in response to dynamic loading and ultrasonic testing.

In this paper, six models (two symmetric models and four total models) with different number of elements for the isotropic and orthotropic inclusions are

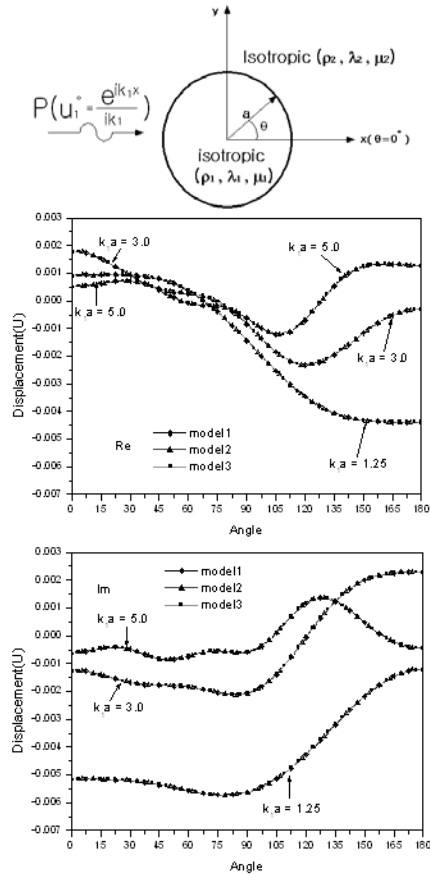


Fig. 4. Real and Imaginary parts of the displacement u_1 (displacement in the x-axis) using VIEM at the interface of single isotropic cylindrical inclusion for $k_1a = 1.25, 3.0$ and $5.0.$ k_1 is the P wavenumber in the unbounded isotropic matrix.

used for the convergence test. The six models are Model 1 (total model with 144 elements), Model 2 (symmetric model with 64 elements), Model 3 (total model with 384 elements), Model 4 (symmetric model with 144 elements), Model 5 (symmetric model with 225 elements) and Model 6 (symmetric model with 289 elements). The VIEM solutions using the different models converged very well within this range of nodal elements. It should be noted that the VIEM solutions for the isotropic inclusion converged more quickly than those for the orthotropic inclusion.

Figs. 4 and 5 show real and imaginary parts of the displacement components, u_1 (along the x-axis) and u_2 (along the y-axis), at the interface of single isotropic cylindrical inclusion using the volume integral equation method for different frequencies. The accuracy of the VIEM solution to this problem was studied and confirmed by Lee and Mal [17].

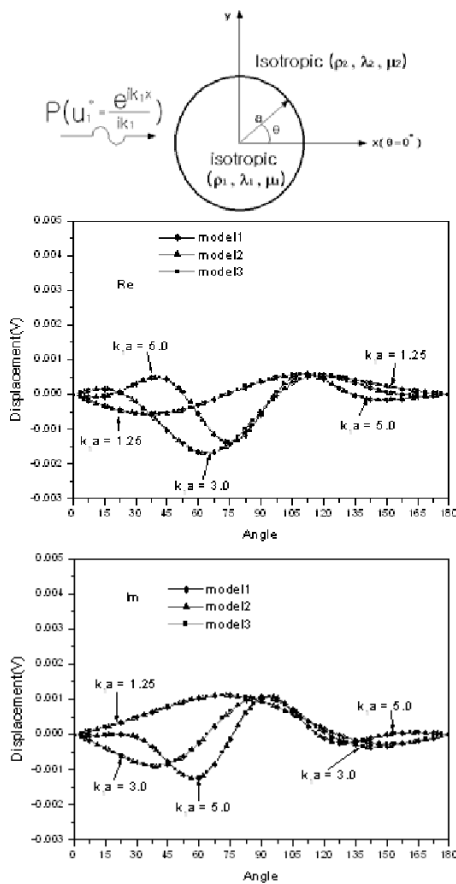


Fig. 5. Real and Imaginary parts of the displacement u_2 (displacement in the y-axis) using VIEM at the interface of single isotropic cylindrical inclusion for $k_1 a = 1.25, 3.0$ and 5.0 . k_1 is the P wavenumber in the unbounded isotropic matrix.

4.2 Scattering of P waves in unbounded isotropic matrix containing an orthotropic inclusion

In order to investigate the difference between an isotropic inclusion and an anisotropic inclusion, we next consider a single orthotropic cylindrical inclusion in the unbounded isotropic matrix as shown in Fig. 6. Fig. 3 shows a typical discretized model used in the VIEM. The unbounded isotropic matrix is assumed to be the same as before. The density and c_{11} for the orthotropic inclusion are assumed to be the same as those of the isotropic inclusion, while the other elastic constants, c_{12}, c_{22} and c_{66} , of the isotropic and orthotropic inclusions are assumed to be different from each other. The elastic constants for the materials of the isotropic matrix and the orthotropic inclusion are listed in Table 1. The incident waves in Eq. (15) with three different normalized wavenumbers,

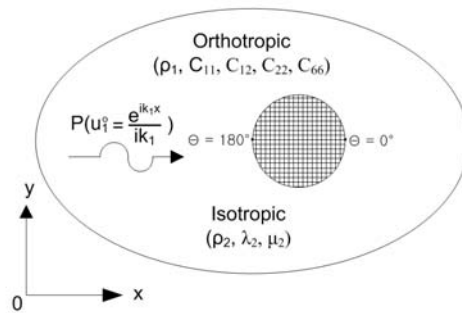


Fig. 6. P wave interaction with an orthotropic inclusion in unbounded isotropic matrix.

$k_1 a = 1.25, 3.0$, and 5.0 , are used as before.

According to the authors' knowledge, neither the analytical solution to this problem nor the closed form solution for the two-dimensional time-harmonic elastodynamic Green's function for the orthotropic material is available in the literature. Thus, comparison between the VIEM solution and the result from the analytical or boundary integral equation method is omitted and the verification for the VIEM result will be replaced with a comparison between the VIEM solution and the results from the analytical and BIEMs to the corresponding elastostatic problem by [14]. Lee et al. [14] considered a single orthotropic elliptic-cylindrical inclusion in the unbounded isotropic matrix under uniform remote tensile loading, σ_X^0 . There was excellent agreement between the analytical solution (see, e.g., [25, 26]) and the numerical solutions using VIEM and BIEM for the normalized tensile stress component (σ_X / σ_X^0) within the orthotropic inclusion under uniform remote tensile loading (σ_X^0) for all cases considered.

Figs. 7 and 8 show real and imaginary parts of the displacements, u_1 and u_2 , at the interface of single orthotropic cylindrical inclusion using the VIEM for different frequencies. The VIEM solutions using the six different models used in Section 4.1 converged more slowly than those for the isotropic inclusion.

Figs. 4, 5, 7 and 8 show that the x-components of the displacement, u_1 , for the isotropic and orthotropic inclusions are not much different from each other. This is due to the fact that the stiffness constant, c_{11} , is the same for the isotropic and orthotropic inclusions. On the other hand, the y-components of the displacement, u_2 , for the two cases are quite different due to the difference in the values of the stiffness constant, c_{22} of the two materials.

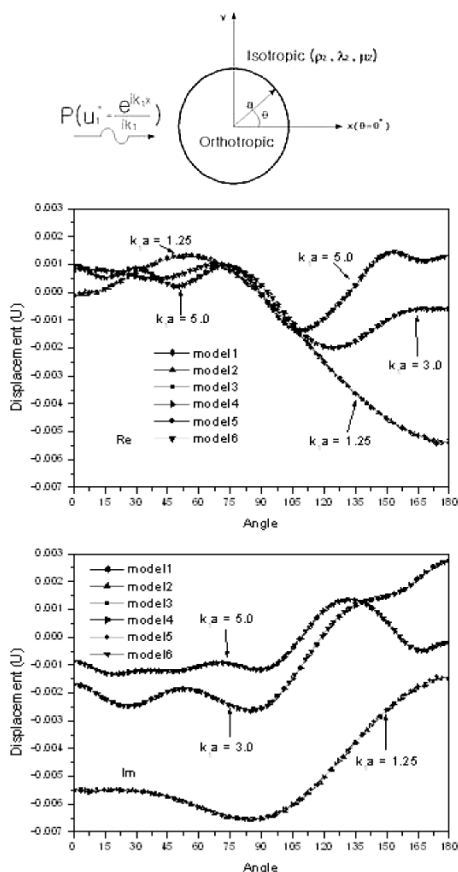


Fig. 7. Real and Imaginary parts of the displacement u_1 (displacement in the x-axis) using VIEM at the interface of single orthotropic cylindrical inclusion for $k_1 a = 1.25, 3.0$ and 5.0 . k_1 is the P wavenumber in the unbounded isotropic matrix.

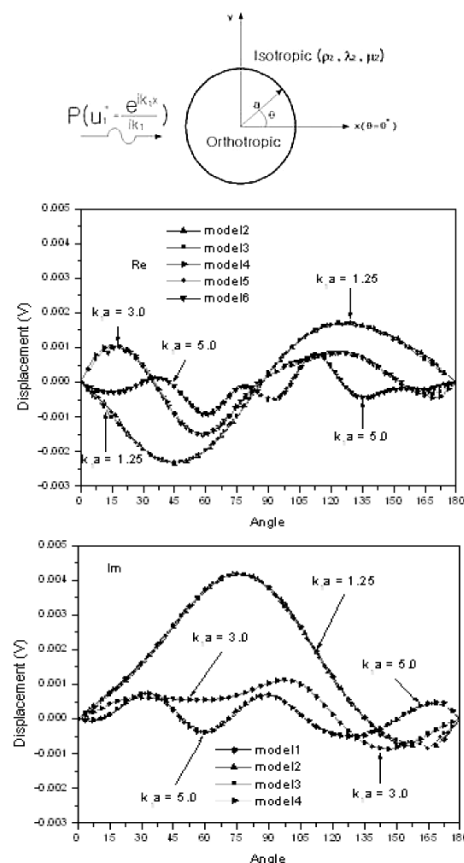


Fig. 8. Real and Imaginary parts of the displacement u_2 (displacement in the y-axis) using VIEM at the interface of single orthotropic cylindrical inclusion for $k_1 a = 1.25, 3.0$ and 5.0 . k_1 is the P wavenumber in the unbounded isotropic matrix.

4.3 Scattering of SV waves in unbounded isotropic matrix containing isotropic and orthotropic inclusions

In the SV wave case the incident wave is assumed to be given by

$$u_2^0 = \frac{e^{ik_2 x}}{ik_2} \tag{16}$$

where k_2 is the S wavenumber in the matrix material (Fig. 9). The normalized wavenumbers, $k_1 a = 1.25, 3.0,$ and $5.0,$ and the elastic constants for the isotropic inclusion are listed in Table 1.

Fig. 10 shows real and imaginary parts of the displacement component, $u_2,$ at the interface of the isotropic cylindrical inclusion at different frequencies.

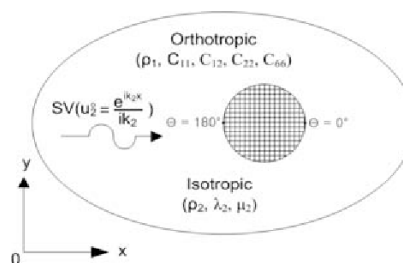


Fig. 9. SV wave interaction with an orthotropic inclusion in unbounded isotropic matrix.

The accuracy of the VIEM solution to this problem was studied and confirmed by Lee and Mal [17]. In order to investigate the difference between an isotropic inclusion and an orthotropic inclusion, a single orthotropic cylindrical inclusion in the unbounded isotropic matrix is considered next. The elastic con-

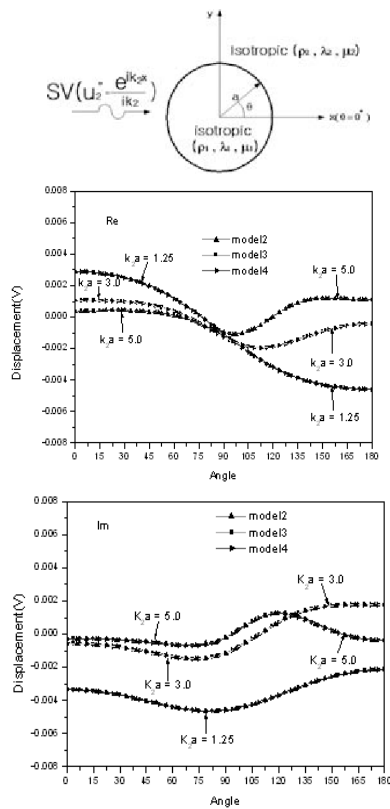


Fig. 10. Real and Imaginary parts of the displacement u_2 (displacement in the y-axis) using VIEM at the interface of single isotropic cylindrical inclusion for $k_2a = 1.25, 3.0$ and 5.0 . k_2 is the S wavenumber in the unbounded isotropic matrix.

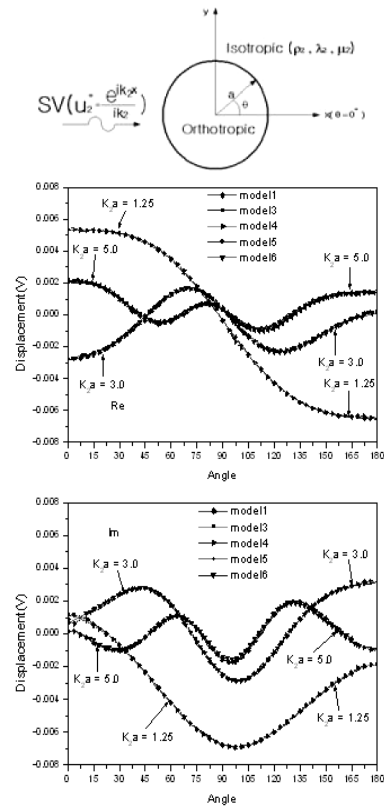


Fig. 11. Real and Imaginary parts of the displacement u_2 (displacement in the y-axis) using VIEM at the interface of single orthotropic cylindrical inclusion for $k_2a = 1.25, 3.0$ and 5.0 . k_2 is the S wavenumber in the unbounded isotropic matrix.

stants for the materials of the isotropic matrix and the orthotropic inclusion are assumed to be the same as before and are listed in Table 1. The convergence of the VIEM solutions was verified by increasing the number of nodes for the models used in Section 4.1. Fig. 11 shows real and imaginary parts of the displacement component, u_2 , at the interface of the orthotropic cylindrical inclusion at different frequencies. Figs. 10, 11 show that, due to the difference in the values of the stiffness constant, c_{22} of the two materials, u_2 , the y-components of the displacement for the isotropic and orthotropic inclusions are very different from each other.

Also, because the stiffness constant, c_{11} , is the same for the isotropic and orthotropic inclusions, the x-component of the displacement, u_1 , for the isotropic and orthotropic inclusions are not much different from each other. Thus, real and imaginary parts of the displacement component, u_1 , at the interface of the isotropic cylindrical inclusion at different frequencies

are not shown here.

5. Multiple inclusion problems

For multiple isotropic or anisotropic inclusions, the volume integral equation method is easier and more convenient to apply than the boundary integral equation method. Since the continuity condition at each interface is automatically satisfied in the volume integral equation formulation, it is not necessary to apply continuity conditions at each interface. Also, there is no change in the basic formulation from the single inclusion case. Furthermore, the method is not sensitive to the geometry of the inclusions.

5.1 Scattering of SH waves in unbounded isotropic matrix containing multiple isotropic inclusions

For SH waves, the volume integral equation (1) becomes

$$u_3(\mathbf{x}) = u_3^0(\mathbf{x}) + \int_R \{ \delta\rho\omega^2 g_3^3(\xi, \mathbf{x}) u_3(\xi) - \delta\mu [g_{3,1}^3 u_{3,1} + g_{3,2}^3 u_{3,2}] \} d\xi_1 d\xi_2 \quad (17)$$

where $u_3(\mathbf{x})$ is the anti-plane displacement component, $\delta\rho = \rho_1 - \rho_2$, $\delta\mu = \mu_1 - \mu_2$, and μ is the shear modulus.

In Eq. (17), $g_i^m(\xi, \mathbf{x})$ is Green's function for the unbounded isotropic matrix material. The Green's function for the SH problem is given by Kitahara [19]

$$g_3^3(x, \xi) = \frac{iH_0(k_2 r)}{4\mu_2} \quad (18)$$

where $r = |\mathbf{x} - \xi|$, $k_2 = \omega/\beta_2$ is the S wavenumber, β_2 is the shear wave speed in the matrix material, and H_0 is the Hankel function of the first kind of the zeroth order. Since the unknowns are the displacements and strains inside the inclusion, it is convenient to discretize this region by using standard finite elements, resulting in a system of linear algebraic equations for the unknown nodal displacements inside the inclusion. The integro-differential equation (17) can, in principle, be solved numerically for multiple isotropic or anisotropic inclusions (see, e.g., Lee and Mal [17]).

In the SH wave case the incident wave is assumed to be given by

$$u_3^0 = e^{ik_2 x} \quad (19)$$

where k_2 is the S wavenumber in the matrix material. The discretized form of Eq. (2) is solved for the unknown $u_3(\mathbf{x})$ and its derivatives within the inclusion.

There is no change in the basic formulation for multiple inclusions from the single inclusion case. In the host medium, $\delta\rho$ and $\delta\mu$ vanish so that it is necessary to discretize the multiple inclusions only. For each observation point, it is necessary to integrate over the whole domain of each inclusion. Although the volume integral equation method can be applied to arbitrary packing sequences and shapes of isotropic or anisotropic inclusions, in order to compare the calculated results with available analytical solutions, simple packing sequence (hexagonal and square) and isotropic circular inclusions in Fig. 12 were considered. The material properties used are those for typical graphite/epoxy composites and are given in Table 2.

Table 2. Material properties of graphite/epoxy composites.

Material	Density(g/cm ³)	μ (GPa)
Graphite	1.79	27.580
Epoxy	1.26	1.595

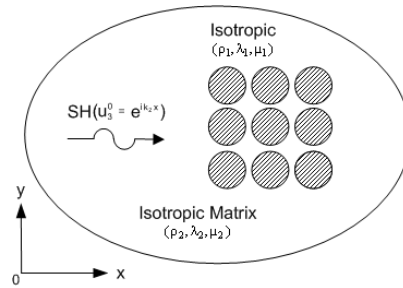
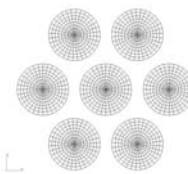
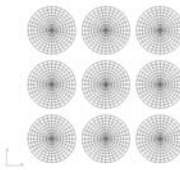


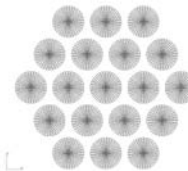
Fig. 12. SH wave interaction with multiple isotropic inclusions.



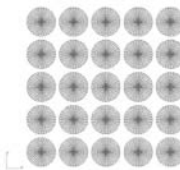
(a) 7 inclusions of hexagonal packing sequence



(b) 9 inclusions of square packing sequence



(c) 19 inclusions of hexagonal packing sequence



(d) 25 inclusions of square packing sequence

Fig. 13 Discretized models for multiple inclusion problems used in the volume integral equation method.

Table 3. Real part of calculated average strains in the central fiber by analytical and volume integral equation methods. The material is graphite/epoxy with volume concentration 0.6 and frequency is 10 MHz.

Number of Inclusions	Average Strain (Re)		
	Analytical	VIE	Difference
7	0.09416	0.09474	0.61%
9	0.09035	0.09048	0.14%
19	0.08072	0.08089	0.21%
25	0.08047	0.08070	0.29%

Table 4. Imaginary part of calculated average strains in the central fiber by analytical and volume integral equation methods. The material is graphite/epoxy with volume concentration 0.6 and frequency is 10 MHz.

Number of Inclusions	Average Strain (Im)		
	Analytical	VIE	Difference
7	-0.0270	-0.0272	0.74%
9	-0.0329	-0.0330	0.30%
19	-0.0519	-0.0523	0.77%
25	-0.0645	-0.0652	1.10%

Fig. 13 shows discretized models used in the VIEM. The standard eight-node quadrilateral and six-node triangular elements were used in the VIEM. The total number of elements for each inclusion used in VIEM was 256.

Tables 3 and 4 show real and imaginary parts of the calculated average strains in the central isotropic fiber by analytical Yang and Mal [27] and the volume integral equation methods for different numbers of inclusions. It can be seen that the percentage differences in the two sets of results are less than 1% in all cases.

6. Concluding remarks

The volume integral equation method is applied to the solution of two-dimensional wave scattering problems with isotropic or anisotropic inclusions in unbounded isotropic matrix. The main advantage of this technique over those based on finite elements is that it requires discretization of the inclusions only in contrast to the need to discretize the entire domain. It is similar to the boundary integral equation method except for the presence of the volume integral over the inclusions instead of the surface integrals over the two sides of the interface. If the medium contains a small number of isotropic inclusions, this method may not have any advantage over BIEM. However, in the presence of multiple non-smooth inclusions, the

BIEM numerical treatment becomes cumbersome. Since standard finite elements are used in the VIEM, it is very easy and convenient to handle multiple non-smooth inclusions. In elastodynamic problems involving multiple anisotropic inclusions, BIEM numerical treatment becomes extremely difficult since closed form expressions for elastodynamic Green's function for anisotropic media are not available.

The formulations developed in this paper can be used to calculate the dynamic stress intensity factors and other quantities of practical interest in realistic models of materials containing strong heterogeneities.

References

- [1] A. J. Niklasson and S. K. Datta, Scattering by an infinite transversely isotropic cylinder in a transversely isotropic medium, *Wave Motion*, 27 (1998) 169-185.
- [2] R. B. Yang and A. K. Mal, Elastic waves in a composite containing inhomogeneous fibers, *International Journal of Engineering Science*, 34 (1) (1996) 67-79.
- [3] T. Chen, Thermoelastic properties and conductivity of composites reinforced by spherically anisotropic particles, *Mechanics of Materials*, 14 (1993) 257-268.
- [4] Z. P. Duan, R. Kienzler, G. Herrmann, An integral equation method and its application to defect mechanics, *Journal of Mechanics and Physics of Solids*, 34 (1986) 539-561.
- [5] W. C. Johnson, Y. Y. Earmme and J. K. Lee, Approximation of the strain field associated with an inhomogeneous precipitate. I: Theory, *Journal of Applied Mechanics - Transactions of the ASME*, 47 (1980) 775-780.
- [6] Z. A. Moschovidis and T. Mura, Two-ellipsoidal inhomogeneities by the equivalent inclusion method, *Journal of Applied Mechanics - Transactions of the ASME*, 42 (1975) 847-852.
- [7] Y. -H. Pao and C. -C. Mow, Diffraction of elastic waves in dynamic stress concentrations, Crane, Russak (& Co.), New York, (1973).
- [8] R. C. McPedran and A. B. Movchan, The Rayleigh multipole method for linear elasticity, *Journal of Mechanics and Physics of Solids*, 42 (1994) 711-727.
- [9] V. I. Kushch, Interacting cracks and inclusions in a solid by multipole expansion method, *International Journal of Solids and Structures*, 35 (1998) 1751-

- 1762.
- [10] A. Sáez and J. Dominguez, BEM analysis of wave scattering in transversely isotropic solids, *Int. J. Numer. Meth. Engng.* 44 (1999) 1283-1300.
- [11] A. Sáez and J. Dominguez, Far field dynamic Green's functions for BEM in transversely isotropic solids, *Wave Motion*, 32 (2000) 113-123.
- [12] C. -Y. Wang and J. D. Achenbach, Three-dimensional time-harmonic elastodynamic Green's functions for anisotropic solids, *Proc. R. Soc. Lond. A*, 449 (1995) 441-458.
- [13] K. J. Lee and A. K. Mal, A boundary element method for plane anisotropic elastic media, *Transactions of the ASME - Journal of Applied Mechanics*, 57 (1990) 600-606.
- [14] J. K. Lee, S. J. Choi and A. Mal, Stress analysis of an unbounded elastic solid with orthotropic inclusions and voids using a new integral equation technique, *Int. J. Solids Structures*, 38 (16) (2001) 2789-2802.
- [15] J. K. Lee, H. M. Lee and A. Mal, A mixed volume and boundary integral equation technique for elastic wave field calculations in heterogeneous materials, *Wave Motion*, 39 (1) (2004) 1–19.
- [16] A. K. Mal and L. Knopoff, Elastic wave velocities in two component systems, *J. Inst. Math. Applics.* 3 (1967) 376-387.
- [17] J. K. Lee and A. K. Mal, A volume integral equation technique for multiple scattering problems in elastodynamics, *Applied Mathematics and Computation*, 67 (1995) 135-159.
- [18] J. K. Lee and A. K. Mal, A volume integral equation technique for multiple inclusion and crack interaction problems, *Transactions of the ASME - Journal of Applied Mechanics*, 64 (1997) 23-31.
- [19] M. Kitahara, Boundary integral equation methods in eigenvalue problems of elastodynamics and thin plates, Elsevier Science Pubs., London and New York, (1985).
- [20] P. K. Banerjee, The boundary element methods in engineering, McGraw-Hill, U.K., (1993).
- [21] F. J. Rizzo, D. J. Shippy, M. Rezayat, A boundary integral equation method for radiation and scattering of elastic waves in three dimensions, *International Journal for Numerical Methods in Engineering*, 21 (1985) 115-129.
- [22] M. Cerrolaza and E. Alarcon, A bi-cubic transformation for the numerical evaluation of the Cauchy principal value integrals in boundary methods, *International Journal for Numerical Methods in Engineering*, 28 (1989) 987-999.
- [23] H. B. Li and G. M. Han, A new method for evaluating singular integrals in stress analysis of solids by the direct boundary element method, *International Journal for Numerical Methods in Engineering*, 21 (1985) 2071-2098.
- [24] S. Lu and T. Q. Ye, Direct evaluation of singular integrals in elastoplastic analysis by the boundary element method, *International Journal for Numerical Methods in Engineering*, 32 (1991) 295-311.
- [25] C. Hwu and W. J. Yen, On the anisotropic elastic inclusions in plane elastostatics, *Journal of Applied Mechanics - Transactions of the ASME*, 60 (1993) 626-632.
- [26] H. C. Yang and Y. T. Chou, , “Generalized plane problems of elastic inclusions in anisotropic solid¹,” *Journal of Applied Mechanics - Transactions of the ASME*, 43 (1976) 424-430.
- [27] R. B. Yang and A. K. Mal, Phase velocity and attenuation of SH waves in a fiber reinforced composite, *Review of Progress in Quantitative Nondestructive Evaluation*, 12A (1993) 155-162.